Mathematical Modelling and Numerical Simulation with Applications, 2023, 3(1), 58–73

https://dergipark.org.tr/en/pub/mmnsa
ISSN Online: 2791-8564 / Open Access
https://doi.org/10.53391/mmnsa.1274004

RESEARCH PAPER

Modelling Influenza A disease dynamics under Caputo–Fabrizio fractional derivative with distinct contact rates

Fırat Evirgen [1,*,‡], **Esmehan Uçar** [1,‡], **Sümeyra Uçar** [1,‡] **and Necati Özdemir** [1,‡]

[1]Department of Mathematics, Faculty of Arts and Sciences, Balıkesir University, 10145 Balıkesir, Türkiye

*Corresponding Author
‡fevirgen@balikesir.edu.tr (Fırat Evirgen); esucarr@gmail.com (Esmehan Uçar); sumeyraucar@balikesir.edu.tr (Sümeyra Uçar); nozdemir@balikesir.edu.tr (Necati Özdemir)

Abstract

The objective of this manuscript is to present a novel approach to modeling influenza A disease dynamics by incorporating the Caputo-Fabrizio (CF) fractional derivative operator into the model. Particularly distinct contact rates between exposed and infected individuals are taken into account in the model under study, and the fractional derivative concept is explored with respect to this component. We demonstrate the existence and uniqueness of the solution and obtain the series solution for all compartments using the Laplace transform method. The reproduction number of the Influenza A model, which was created to show the effectiveness of different contact rates, was obtained and examined in detail in this sense. To validate our approach, we applied the predictor-corrector method in the sense of the Caputo-Fabrizio fractional derivative and demonstrate the effectiveness of the fractional derivative in accurately predicting disease dynamics. Our findings suggest that the use of the Caputo-Fabrizio fractional derivative can provide valuable insights into the mechanisms underlying influenza A disease and enhance the accuracy of disease models.

Keywords: Fractional differential equations; fixed point theory; Caputo-Fabrizio derivative; influenza

AMS 2020 Classification: 34A08; 34A34; 93A30

1 Introduction

Influenza is an infectious respiratory disease caused by a single-stranded and segmented RNA virus in the Orthomyxoviridae family. Influenza is commonly known as "the flu". It has 3 different types, namely A, B, and C, and the type of virus responsible for large epidemics with high mortality

➤ **Received:** 14.02.2023 ➤ **Revised:** 25.03.2023 ➤ **Accepted:** 27.03.2023 ➤ **Published:** 31.03.2023

is often Influenza A. Influenza A viruses infect a range of mammalian (e.g. pigs and horses) and avian species, whereas type B and C infections are largely restricted to humans. Within this group of types, only types A and B are capable of causing severe illnesses in humans. Two glycoproteins, hemagglutinin (H) and neuraminidase (N), located on the outside of the viral particle, are used in the classification of influenza viruses. All 18 H and 11 R subtypes of influenza A viruses have been isolated from nature and described in the literature [1]. H1N1, H1N2, H2N2, H3N1, and others can be given as examples of this nomenclature. Like humans, every living thing has its own influenza virus. Influenza viruses in animals can be transmitted to humans and cause a pandemic that affects the whole world. The most important of these is the H1N1 subtype of influenza A, which caused the Spanish flu pandemic in 1918, the Russian flu pandemic in 1977, and the swine flu pandemic in 2009 [2]. These viruses lose their ability to cause an epidemic that will affect the whole world within a few years and take their place among seasonal influenza agents in the following years. Influenza viruses can easily be transmitted from sick people to other people, and the disease reaches its peak during the winter months when people spend more time indoors. Influenza is usually transmitted by the behavior of people who are sick, such as talking, coughing, and sneezing. More rarely, it can be transmitted by touching surfaces, tools, and equipment contaminated with virus-containing droplets. The flu is mild in many people and these people recover completely within a few days. However, it has a severe course in the elderly, young children, immune-deficient persons, and those with chronic diseases, and may cause hospitalizations and even death. This disease can cause a wide range of symptoms, ranging from mild to severe, including fever, sore throat, runny nose, headache, muscle pain, coughing, and fatigue, among others. Although drugs are used in the treatment of influenza, scientific studies have shown that the most effective way to prevent the disease is vaccination. However, the continuous mutation of the influenza virus requires that the vaccine be updated every year in order to be protected from the disease.

The course and effects of the disease can also be examined theoretically with mathematical models that will be created in the presence of up-to-date data. In addition, the fractional derivative concept has been adapted to add the memory effect to the mathematical models. Thereby, the instantaneous behavior of the dynamic system can be depicted with the effect of past accumulations. In this regard, many mathematical models, including integer and fractional order, have been created in the literature for the detailed analysis of various diseases such as cancer cells [3–5], varicella zoster virus [6], COVID-19 [7–9], plant disease [10], diabetes [11], prey-predator model [12], Nipah virus [13], childhood diseases [14], and hepatitis B [15]. Additionally, several studies have also been conducted regarding fractional derivative applications in various fields, such as optimal control [16, 17], fixed point theory [18–20], chaotic systems [21], and heat flow [22]. In the same way, a number of mathematical models developed in regard to influenza have attempted to contribute to the literature in this area. In 2004 Alexander et al. [23] created an SVIRS model and determined the threshold limit for vaccination, in order to reduce the spread of influenza in the community. Casagrandi et al. [24] adapted cross-immune individuals to the classical SIR model and examined its effects on the course of the disease. The transmission of the influenza virus between bird and human populations has been discussed in detail by the proposed model in [25]. With the model created in 2010 [26], the effects of wearing N95 and surgical masks on influenza were revealed with quantitative analyzes. To explain and understand the outbreaks of influenza A (H1N1), a nonlinear fractional order model is constructed in the Caputo sense [27], and the results are compared with the real data from 2009. A new model describing the transmission of the influenza virus by disease resistance in humans has been introduced in [28] and disease equilibrium points have been determined and stability analyses have been carried out. Furthermore, Jia and Xiao [29] discussed this model with nonlinear incidence rates. Partial differential equations have been

used in the study [30] to assess the impact of diffusion and advection on influenza A virus kinetics and localization in the human respiratory tract. Srivastava et al. [31] investigated the effect of the influenza virus on a cellular basis on a fractional order model, taking into account the components of the human immune system as antibodies, plasma cells, effector cells, and interferon. In [32] the authors, the influenza mathematical model is handled by considering two strains with two different incidence rates. The effects of COVID-19 and influenza diseases on each other were examined on a deterministic co-infection model created by Ojo et al. [33]. In addition, various control strategies have been developed with 3 control parameters added to the model. The course and quantitative analysis of the influenza A virus under the newly defined fractal-fractional operator is discussed in [34]. Derradji et al. [35] presented a fractional SEIRS model in the sense of Caputo-Fabrizio with disease resistance and a nonlinear generalized incidence rate. An influenza disease model with a cross-immune population was remodeled under the effect of the fractional order derivative and solved by the stochastic Levenberg-Marquardt backpropagation neural networks [36].

This study was motivated by the need to better understand the spread of influenza A, leading to the creation of an integer-order model. The model incorporates a novel approach whereby the contact rate for each exposed and infected individual is treated separately. Additionally, the model incorporates the use of the Caputo-Fabrizio fractional derivative operator.

This paper is organized in the following manner. In Section 2, some basic definitions of fractional calculus, which form the basis of the study, are reminded. In Section 3, the components of the proposed integer and fractional models and their biological meanings are described. The existence and uniqueness of the solution of the model under the CF derivative are detailed in Section 4. In Section 5, it is theoretically proven that the model components have a series solution using the Laplace transformed method. The effectiveness of contact rates corresponding to exposed and infected individuals on the reproduction number is discussed in Section 6. The effect of fractional derivatives of different order on the course of influenza disease is illustrated in Section 7. Moreover, in these simulations, the behavior of some model parameters under the fractional derivative was also examined in detail. Finally, the results are expressed in the conclusion section.

2 Some preliminaries

Here, we recall some fundamental notions.

Definition 1 *[37] Let $a < b, g \in H^1(a,b)$ and $\sigma \in (0,1)$, the Caputo-Fabrizio (CF) derivative is*

$$ {}^{CF}D_t^{\sigma}[g(t)] = \frac{F(\sigma)}{1-\sigma}\int_a^t g'(x)\exp\left[-\sigma\frac{(t-x)}{1-\sigma}\right]dx, $$

where $F(\sigma)$ is a normalization function and $F(0) = F(1) = 1$.

Definition 2 *[38] Let $\sigma \in (0,1)$. The fractional integral related to the CF derivative is defined by:*

$$ {}^{CF}I_t^{\sigma}[g(t)] = \frac{1-\sigma}{F(\sigma)}g(t) + \frac{\sigma}{F(\sigma)}\int_a^t g(\lambda)\,d\lambda. $$

Definition 3 *[38] The Laplace transform of CF derivative can be given*

$$ \mathfrak{L}\left[{}^{CF}D_t^{\sigma}[g(t)]\right] = \frac{s\mathfrak{L}[g(t)]}{s+\sigma(1-s)} - \frac{g(0)}{s+\sigma(1-s)}. $$

3 Mathematical model of Influenza A

In this section, an SEIRS model was developed by taking into account separate contact rates for exposed and infected individuals, as inspired by previous research [28, 29, 35]. The model compartments and the biological meanings of the parameters can be seen as follows:

$$\begin{aligned}
\frac{dS(t)}{dt} &= \Lambda - \gamma_1 S(t) E(t) - \gamma_2 S(t) I(t) + cE(t) + bI(t) + \alpha R(t) - \mu S(t), \\
\frac{dE(t)}{dt} &= \gamma_1 S(t) E(t) + \gamma_2 S(t) I(t) - (c + \varepsilon + \mu) E(t), \\
\frac{dI(t)}{dt} &= \varepsilon E(t) - (\beta + b + \mu) I(t), \\
\frac{dR(t)}{dt} &= \beta I(t) - (\alpha + \mu) R(t),
\end{aligned} \tag{1}$$

where $S(t)$ represents the number of susceptible individuals, $E(t)$ represents the number of exposed individuals, $I(t)$ represents the number of infected individuals, $R(t)$ represents the number of recovered individuals, Λ is a constant recruitment ratio of susceptible humans, γ_1 is the transmission rate of viruses by contact between susceptible and exposed individuals, γ_2 is the transmission rate of viruses by contact between susceptible and infected individuals, the rate at which an exposed person develops susceptibility without therapy is c, b is the rate at which an infected person develops into a susceptible person in the absence of therapy, $\varepsilon = \frac{1}{IIP}$ where IIP stands for the virus's intrinsic incubation period, the rate at which a recovered person becomes a vulnerable person once more is denoted by the symbol α, β is the rate at which the infectious person becomes to be the recovered person, and the population's natural death rate is expressed by the symbol μ.

The use of fractional derivatives in mathematical modeling has become increasingly popular in recent years. One of these fractional derivative definitions is the Caputo-Fabrizio fractional derivative which is a modification of the classical Caputo derivative by using an additional parameter to account for the non-locality of the fractional derivative. This additional parameter can help to better capture the complex behavior of real-world systems, such as in the spread of infectious diseases, where the contact rate between infected and susceptible individuals may vary over time and make more accurate predictions about their future behavior. Now, by replacing the time derivative with the CF fractional derivative operator, we moderate the system. As a result of this change, the dimensions on the right-hand side and the left-hand side of the page will differ. In order to resolve this issue, we adjust the fractional operator so that the sides are of the same dimension using an auxiliary parameter called κ [39]. Based on these explanations and CF fractional derivative, the model (1) take the following form:

$$\begin{aligned}
\kappa^{\sigma-1} {}^{CF}D_t^{\sigma} S(t) &= \Lambda - \gamma_1 S(t) E(t) - \gamma_2 S(t) I(t) + cE(t) + bI(t) + \alpha R(t) - \mu S(t), \\
\kappa^{\sigma-1} {}^{CF}D_t^{\sigma} E(t) &= \gamma_1 S(t) E(t) + \gamma_2 S(t) I(t) - (c + \varepsilon + \mu) E(t), \\
\kappa^{\sigma-1} {}^{CF}D_t^{\sigma} I(t) &= \varepsilon E(t) - (\beta + b + \mu) I(t), \\
\kappa^{\sigma-1} {}^{CF}D_t^{\sigma} R(t) &= \beta I(t) - (\alpha + \mu) R(t),
\end{aligned} \tag{2}$$

with the initial conditions $S(0) = S_0 \geq 0$, $E(0) = E_0 \geq 0$, $I(0) = I_0 \geq 0$ and $R(0) = R_0 \geq 0$.

4 Existence of solution

A natural question one might ask is whether the model we construct in order to describe a physical phenomenon appears accurate enough. In order to guarantee this, we can apply the theory of fixed points to our problem. We therefore use the aforementioned theory to demonstrate the existence of the solution for the relevant model (2).

$$\begin{aligned}
\Psi_1(t,S,E,I,R) &= \kappa^{1-\sigma}\left(\Lambda-\gamma_1 S(t)E(t)-\gamma_2 S(t)I(t)+cE(t)+bI(t)+\alpha R(t)-\mu S(t)\right),\\
\Psi_2(t,S,E,I,R) &= \kappa^{1-\sigma}\left(\gamma_1 S(t)E(t)+\gamma_2 S(t)I(t)-(c+\varepsilon+\mu)E(t)\right),\\
\Psi_3(t,S,E,I,R) &= \kappa^{1-\sigma}\left(\varepsilon E(t)-(\beta+b+\mu)I(t)\right),\\
\Psi_4(t,S,E,I,R) &= \kappa^{1-\sigma}\left(\beta I(t)-(\alpha+\mu)R(t)\right).
\end{aligned} \tag{3}$$

Applying the operator ${}^{CF}I_t^{\sigma}$ to the model (2) on both sides, we have

$$\begin{aligned}
S(t) &= S(0)+{}^{CF}I_t^{\sigma}\left[\Psi_1(t,S,E,I,R)\right],\\
E(t) &= E(0)+{}^{CF}I_t^{\sigma}\left[\Psi_2(t,S,E,I,R)\right],\\
I(t) &= I(0)+{}^{CF}I_t^{\sigma}\left[\Psi_3(t,S,E,I,R)\right],\\
R(t) &= R(0)+{}^{CF}I_t^{\sigma}\left[\Psi_4(t,S,E,I,R)\right].
\end{aligned} \tag{4}$$

Considering the right-hand side of the Eq. (4), we achieve

$$U(t)=U_0(t)+\frac{1-\sigma}{M(\sigma)}\left[\Psi(t,U(t))-\Psi_0(t)\right]+\frac{\sigma}{M(\sigma)}\int_0^t \Psi(\theta,U(\theta))\,d\theta, \tag{5}$$

where

$$U(t)=\begin{cases} S(t)\\ E(t)\\ I(t)\\ R(t)\end{cases},\quad U_0(t)=\begin{cases} S(0)\\ E(0)\\ I(0)\\ R(0)\end{cases},\quad \Psi(t,U(t))=\begin{cases} \Psi_1(t,S,E,I,R)\\ \Psi_2(t,S,E,I,R)\\ \Psi_3(t,S,E,I,R)\\ \Psi_4(t,S,E,I,R)\end{cases}. \tag{6}$$

Let

$$B_i=\sup_{t\in[t-d,t+d]}\left\|\Psi_i(t,S,E,I,R)\right\|,\ \text{for } i=1,2,3,4$$

and

$$C[d,b_i]=[t-d,t+d]\times[u-c_i,u+c_i]=D\times D_i \text{ for } i=1,2,3,4.$$

Suppose that a norm on $C[d,b_i]$ for $i=1,2,3,4$ as follows:

$$\left\|U(t)\right\|_{\infty}=\sup_{t\in[t-d,t+d]}\left|U(t)\right|. \tag{7}$$

Consider the Picard operator

$$\theta : C\left(D, D_1, D_2, D_3, D_4\right) \to C\left(D, D_1, D_2, D_3, D_4\right),$$

given as

$$\theta U\left(t\right) = U_0\left(t\right) + \frac{1-\sigma}{M\left(\sigma\right)}\Psi\left(t, U\left(t\right)\right) + \frac{\sigma}{M\left(\sigma\right)}\int_0^t \Psi\left(s, U\left(s\right)\right) ds. \tag{8}$$

Suppose that the solutions of the model Eq. (2) are bounded within a time period, that is

$$\|U\| \leq \max\{d_1, d_2, d_3, d_4\}. \tag{9}$$

Supposing that $d = \frac{1+\sigma t_0}{M(\sigma)}$, $B = \max\{B_i\}$ for $i = 1, 2, 3, 4$ and $t_0 = \max\{t \in D\}$

$$\begin{aligned}
\|\theta U\left(t\right) - U_0\left(t\right)\| &= \sup_{t\in D}\left|\frac{1-\sigma}{M\left(\sigma\right)}\Psi\left(t, U\left(t\right)\right) + \frac{\sigma}{M\left(\sigma\right)}\int_0^t \Psi\left(s, U\left(s\right)\right) ds\right| \\
&\leq \frac{1-\sigma}{M\left(\sigma\right)}\sup_{t\in D}\left|\Psi\left(t, U\left(t\right)\right)\right| + \frac{\sigma}{M\left(\sigma\right)}\sup_{t\in D}\left|\int_0^t \Psi\left(s, U\left(s\right)\right) ds\right| \\
&\leq \left(\frac{1-\sigma}{M\left(\sigma\right)} + \frac{\sigma}{M\left(\sigma\right)}\right) B \\
&\leq \left(\frac{1+\sigma\left(t_0 - 1\right)}{M\left(\sigma\right)}\right) B \\
&< dB \\
&\leq \bar{d},
\end{aligned} \tag{10}$$

which satisfies $d < \frac{\bar{d}}{B}$. Now, we consider the following inequality:

$$\|\theta U_1 - \theta U_2\| = \sup_{t\in D}\left|U_1 - U_2\right|. \tag{11}$$

$$\begin{aligned}
\|\theta U_1 - \theta U_2\| &= \sup_{t\in D}\left|\frac{1-\sigma}{M\left(\sigma\right)}\left(\Psi\left(s, U_1\left(t\right)\right) - \Psi\left(s, U_2\left(t\right)\right)\right)\right. \\
&\quad \left. + \frac{\sigma}{M\left(\sigma\right)}\int_0^t \left(\Psi\left(s, U_1\left(s\right)\right) - \Psi\left(s, U_2\left(s\right)\right)\right) ds\right| \\
&\leq \frac{1-\sigma}{M\left(\sigma\right)}k_1\left|U_1\left(t\right) - U_2\left(t\right)\right| + \frac{\sigma}{M\left(\sigma\right)}k_1\int_0^t \left|U_1\left(s\right) - U_2\left(s\right)\right| ds \\
&\leq \left(\frac{1-\sigma}{M\left(\sigma\right)}k_1 + \frac{\sigma k_1}{M\left(\sigma\right)}t_0\right)\left|U_1 - U_2\right| \\
&\leq dk_1\left|U_1 - U_2\right|,
\end{aligned}$$

where $k_1 < 1$. Since Ψ is a contraction, then we have $k_1 d < 1$. Thus, the operator θ is contraction. So the model (2) has a unique solution.

5 General algorithm for the fractional model

In this section, we give a series solution for our fractional model. Applying Laplace transform to the model (2), we find

$$\begin{aligned}
\mathfrak{L}\left[S\left(t\right)\right]-S\left(0\right) &= \frac{s+\sigma\left(1-s\right)}{s}\mathfrak{L}\left[\begin{array}{c}\kappa^{1-\sigma}\left(\Lambda-\gamma_1 S\left(t\right)E\left(t\right)-\gamma_2 S\left(t\right)I\left(t\right)\right.\\ \left.+cE\left(t\right)+bI\left(t\right)+\alpha R\left(t\right)-\mu S\left(t\right)\right)\end{array}\right],\\
\mathfrak{L}\left[E\left(t\right)\right]-E\left(0\right) &= \frac{s+\sigma\left(1-s\right)}{s}\mathfrak{L}\left[\kappa^{1-\sigma}\left(\gamma_1 S\left(t\right)E\left(t\right)+\gamma_2 S\left(t\right)I\left(t\right)-\left(c+\varepsilon+\mu\right)E\left(t\right)\right)\right],\\
\mathfrak{L}\left[I\left(t\right)\right]-I\left(0\right) &= \frac{s+\sigma\left(1-s\right)}{s}\mathfrak{L}\left[\kappa^{1-\sigma}\left(\varepsilon E\left(t\right)-\left(\beta+b+\mu\right)I\left(t\right)\right)\right],\\
\mathfrak{L}\left[R\left(t\right)\right]-R\left(0\right) &= \frac{s+\sigma\left(1-s\right)}{s}\mathfrak{L}\left[\kappa^{1-\sigma}\left(\beta I\left(t\right)-\left(\alpha+\mu\right)R\left(t\right)\right)\right].
\end{aligned} \tag{12}$$

Take into account the series solution in the shape of:

$$\begin{aligned}
S\left(t\right) &= \sum_{p=0}^{\infty} S_p\left(t\right),\ E\left(t\right) = \sum_{p=0}^{\infty} E_p\left(t\right),\\
I\left(t\right) &= \sum_{p=0}^{\infty} I_p\left(t\right),\ R\left(t\right) = \sum_{p=0}^{\infty} R_p\left(t\right).
\end{aligned} \tag{13}$$

Moreover, the nonlinear terms $E\left(t\right)S\left(t\right)$ and $I\left(t\right)S\left(t\right)$ are decomposed in form of polynomials:

$$E\left(t\right)S\left(t\right) = \sum_{p=0}^{\infty} A_p\left(E,S\right),\ I\left(t\right)S\left(t\right) = \sum_{p=0}^{\infty} B_p\left(I,S\right),$$

where the "Adomian polynomial" $A_p\left(E,S\right)$ may be defined as:

$$A_p\left(E,S\right) = \frac{1}{p!}\frac{d^p}{d\lambda^p}\left[\sum_{i=0}^{p}\lambda^i E_i\left(t\right)\sum_{i=0}^{p}\lambda^i S_i\left(t\right)\right]\Bigg|_{\lambda=0}.$$

In a similar way, the polynomial B_p can be given. The system (12) can be converted to

$$\mathfrak{L}\left[\sum_{p=0}^{\infty} S_p\left(t\right)\right] = \frac{S(0)}{s}+\frac{s+\sigma(1-s)}{s}\mathfrak{L}\left[\kappa^{1-\sigma}\left(\begin{array}{c}\Lambda-\gamma_1\sum_{p=0}^{\infty}A_p\left(E,S\right)-\gamma_2\sum_{p=0}^{\infty}B_p\left(I,S\right)+c\sum_{p=0}^{\infty}E_p\left(t\right)\\ +b\sum_{p=0}^{\infty}I_p\left(t\right)+\alpha\sum_{p=0}^{\infty}R_p\left(t\right)-\mu\sum_{p=0}^{\infty}S_p\left(t\right)\end{array}\right)\right],$$

$$\mathfrak{L}\left[\sum_{p=0}^{\infty} E_p\left(t\right)\right] = \frac{E(0)}{s}+\frac{s+\sigma(1-s)}{s}\mathfrak{L}\left[\kappa^{1-\sigma}\left(\begin{array}{c}\gamma_1\sum_{p=0}^{\infty}A_p\left(E,S\right)+\gamma_2\sum_{p=0}^{\infty}B_p\left(I,S\right)\\ -\left(c+\varepsilon+\mu\right)\sum_{p=0}^{\infty}E_p\left(t\right)\end{array}\right)\right],$$

$$\begin{aligned}
\mathfrak{L}\left[\sum_{k=0}^{\infty} I_p(t)\right] &= \frac{I(0)}{s} + \frac{s+\sigma(1-s)}{s}\mathfrak{L}\left[\kappa^{1-\sigma}\left(\varepsilon\sum_{p=0}^{\infty} E_p(t) - (\beta+b+\mu)\sum_{p=0}^{\infty} I_p(t)\right)\right], \\
\mathfrak{L}\left[\sum_{p=0}^{\infty} R_p(t)\right] &= \frac{R(0)}{s} + \frac{s+\sigma(1-s)}{s}\mathfrak{L}\left[\kappa^{1-\sigma}\left(\beta\sum_{p=0}^{\infty} I_p(t) - (\alpha+\mu)\sum_{p=0}^{\infty} R_p(t)\right)\right]. \qquad (14)
\end{aligned}$$

Now comparing both sides (14) term by term, we have

$$\begin{aligned}
&\mathfrak{L}[S_0(t)] = \frac{S_0}{s}, \mathfrak{L}[E_0(t)] = \frac{E_0}{s}, \mathfrak{L}[I_0(t)] = \frac{I_0}{s}, \mathfrak{L}[R_0(t)] = \frac{R_0}{s}. \\
&\mathfrak{L}[S_1(t)] = \frac{s+\sigma(1-s)}{s}\mathfrak{L}\left[\kappa^{1-\sigma}\left(\lambda - \gamma_1 A_0(E,S) - \gamma_2 B_0(I,S) - cE_0 + bI_0 + \alpha R_0 - \mu S_0\right)\right], \\
&\mathfrak{L}[E_1(t)] = \frac{s+\sigma(1-s)}{s}\mathfrak{L}\left[\kappa^{1-\sigma}\left(\gamma_1 A_0(E,S) + \gamma_2 B_0(I,S) - (c+\varepsilon+\mu)E_0\right)\right], \\
&\mathfrak{L}[I_1(t)] = \frac{s+\sigma(1-s)}{s}\mathfrak{L}\left[\kappa^{1-\sigma}\left(\varepsilon E_0 - (\beta+b+\mu)I_0\right)\right], \\
&\mathfrak{L}[R_1(t)] = \frac{s+\sigma(1-s)}{s}\mathfrak{L}\left[\kappa^{1-\sigma}\left(\beta I_0 - (\alpha+\mu)R_0\right)\right], \\
&\mathfrak{L}[S_2(t)] = \frac{s+\sigma(1-s)}{s}\mathfrak{L}\left[\kappa^{1-\sigma}\left(\Lambda - \gamma_1 A_1(E,S) - \gamma_2 B_1(I,S) - cE_1 + bI_1 + \alpha R_1 - \mu S_1\right)\right], \\
&\mathfrak{L}[E_2(t)] = \frac{s+\sigma(1-s)}{s}\mathfrak{L}\left[\kappa^{1-\sigma}\left(\gamma_1 A_1(E,S) + \gamma_2 B_1(I,S) - (c+\varepsilon+\mu)E_1\right)\right], \\
&\mathfrak{L}[I_2(t)] = \frac{s+\sigma(1-s)}{s}\mathfrak{L}\left[\kappa^{1-\sigma}\left(\varepsilon E_1 - (\beta+b+\mu)I_1\right)\right], \\
&\mathfrak{L}[R_2(t)] = \frac{s+\sigma(1-s)}{s}\mathfrak{L}\left[\kappa^{1-\sigma}\left(\beta I_1 - (\alpha+\mu)R_1\right)\right], \\
&\qquad\vdots \\
&\mathfrak{L}\left[S_{p+1}(t)\right] = \frac{s+\sigma(1-s)}{s}\mathfrak{L}\left[\kappa^{1-\sigma}\left(\gamma_1 A_p(E,S) - \gamma_2 B_p(I,S) - cE_p + bI_p + \alpha R_p - \mu S_p\right)\right], \\
&\mathfrak{L}\left[E_{p+1}(t)\right] = \frac{s+\sigma(1-s)}{s}\mathfrak{L}\left[\kappa^{1-\sigma}\left(\Lambda - \gamma_1 A_p(E,S) + \gamma_2 B_p(I,S) - (c+\varepsilon+\mu)E_p\right)\right], \\
&\mathfrak{L}\left[I_{p+1}(t)\right] = \frac{s+\sigma(1-s)}{s}\mathfrak{L}\left[\kappa^{1-\sigma}\left(\varepsilon E_p - (\beta+b+\mu)I_p\right)\right], \\
&\mathfrak{L}\left[R_{p+1}(t)\right] = \frac{s+\sigma(1-s)}{s}\mathfrak{L}\left[\kappa^{1-\sigma}\left(\beta I_p - (\alpha+\mu)R_p\right)\right],\ p \geq 0. \qquad (15)
\end{aligned}$$

Implementing the inverse Laplace transform to Eq. (15), we obtain

$$\begin{aligned}
&S_0(t) = S_0, E_0(t) = E_0, I_0(t) = I_0, R_0(t) = R_0. \\
&S_1(t) = \left[\kappa^{1-\sigma}\left(\Lambda - \gamma_1 A_0(E,S) - \gamma_2 B_0(I,S) - cE_0 + bI_0 + \alpha R_0 - \mu S_0\right)\right](1+\sigma(t-1)), \\
&E_1(t) = \left[\kappa^{1-\sigma}\left(\gamma_1 A_0(E,S) + \gamma_2 B_0(I,S) - (c+\varepsilon+\mu)E_0\right)\right](1+\sigma(t-1)), \\
&I_1(t) = \left[\kappa^{1-\sigma}\left(\varepsilon E_0 - (\beta+b+\mu)I_0\right)\right](1+\sigma(t-1)), \\
&R_1(t) = \left[\kappa^{1-\sigma}\left(\beta I_0 - (\alpha+\mu)R_0\right)\right](1+\sigma(t-1)), \qquad (16) \\
&\quad\vdots
\end{aligned}$$

Continuing in the same direction, we acquire the other terms. The desired outcome can be stated as:

$$S(t)=\sum_{p=0}^{\infty}S_p(t),E(t)=\sum_{p=0}^{\infty}E_p(t),$$
$$I(t)=\sum_{p=0}^{\infty}I_p(t),R(t)=\sum_{p=0}^{\infty}R_p(t). \tag{17}$$

6 Reproduction number

The reproduction number, denoted as R_0, is a mathematical term that is commonly used in epidemiology to represent the average number of people that one infected person will transmit a disease to in a population where everyone is susceptible to the disease, in the absence of any interventions like vaccines or treatment. The R_0 is determined by using the Next Generation Matrix Method (NGMM) [40, 41]. Firstly, the right side of the model (2) is considered as $\mathcal{F}$-$\mathcal{V}$, where $\mathcal{F}$ and $\mathcal{V}$ demonstrate the transmission part and the transition part, as follow respectively

$$\mathcal{F}=\kappa^{1-\sigma}\begin{pmatrix}E\,S\,\gamma_1+I\,S\,\gamma_2\\0\end{pmatrix}\quad\text{and}\quad\mathcal{V}=\kappa^{1-\sigma}\begin{pmatrix}E\,(c+\varepsilon+\mu)\\I\,(b+\beta+\mu)-E\,\varepsilon\end{pmatrix}.$$

Then, if the Jacobian matrices of the $\mathcal{F}$ and $\mathcal{V}$ are calculated according to the E and I compartments and written instead of the disease-free equilibrium point $\mathcal{E}_0=(S,E,I,R)=\left(\frac{\Lambda}{\mu},0,0,0\right)$ of the model, we get

$$\mathbb{F}=\kappa^{1-\sigma}\begin{pmatrix}\frac{\Lambda\,\gamma_1}{\mu}&\frac{\Lambda\,\gamma_2}{\mu}\\0&0\end{pmatrix}\quad\text{and}\quad\mathbb{V}=\kappa^{1-\sigma}\begin{pmatrix}c+\varepsilon+\mu&0\\-\varepsilon&b+\beta+\mu\end{pmatrix}.$$

Thus, the next generation matrix $\left(\mathbb{F}\mathbb{V}^{-1}\right)$ of the model (2) is obtained and its spectral radius gives the reproduction number R_0 as follow:

$$\mathbb{F}\mathbb{V}^{-1}=\begin{pmatrix}0\\\frac{\Lambda\,(b\,\gamma_1+\beta\,\gamma_1+\varepsilon\,\gamma_2+\gamma_1\,\mu)}{\mu\,(b+\beta+\mu)\,(c+\varepsilon+\mu)}\end{pmatrix}\rightarrow R_0=\frac{\Lambda\,(b\,\gamma_1+\beta\,\gamma_1+\varepsilon\,\gamma_2+\gamma_1\,\mu)}{\mu\,(b+\beta+\mu)\,(c+\varepsilon+\mu)}.$$

The critical value of contact rate refers to the threshold value of the average number of people that an infected individual comes into contact with per day, below which the reproduction number remains below 1. In other words, if the contact rate is lower than the critical value, then the disease will not spread widely in the population. In Figure 1 (a)-(b), the critical value of the contact rates is calculated as $\gamma_1=0.4637$ and $\gamma_2=0.72$ for the model (2). If the average number of contacts per exposed individual is less than 0.4637 and the average number of contacts per infected individual is less than 0.72, then the disease will not spread widely and the outbreak will be contained. However, if the contact rates γ_1 and γ_2 exceed the critical values, then the reproduction number will be greater than 1, and the disease will continue to spread in the population. This highlights the importance of public health measures such as social distancing, mask-wearing, and limiting large gatherings, which can reduce the contact rate and help bring the reproduction number below 1, leading to a decline in the number of new infections. In addition, the change in R_0 can also be observed in Figure 2 depending on the value of γ_1 and γ_2 that have been fixed in the range of 0 to

2. According to this simulation, γ_1 appears to spread the disease more effectively than γ_2, and considering the levels that R_0 can reach, it seems that influenza disease may have the potential to cause a pandemic again in the world in the future.

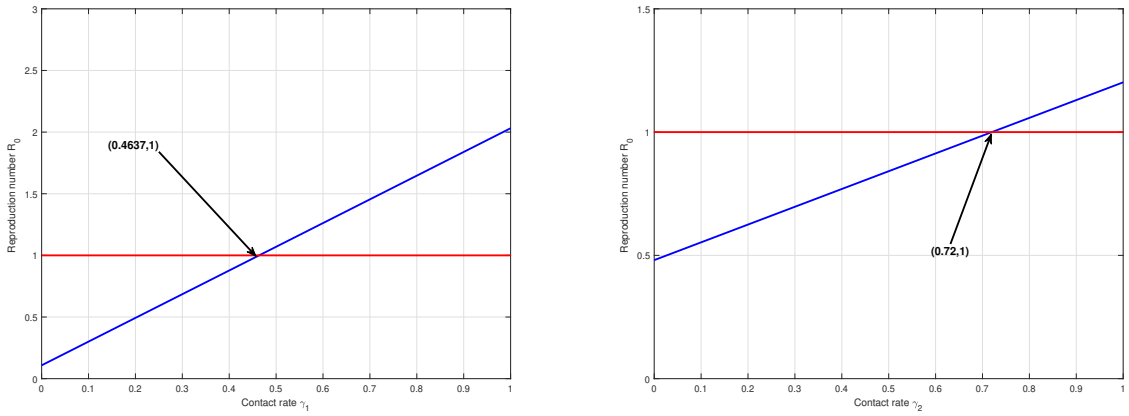

(a) γ_2 fixed as 0.15. **(b)**γ_1 fixed as 0.25.

Figure 1. The critical values of the contact rate γ_1 and γ_2 for the threshold value of $R_0 = 1$.

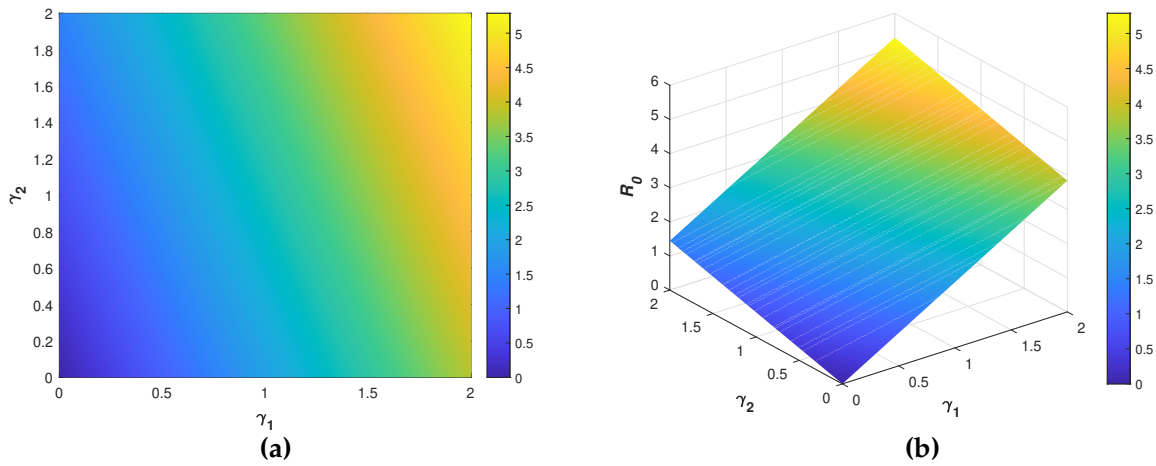

(a) **(b)**

Figure 2. Visualization of the variation in the reproduction number R_0 according to contact rates γ_1 and γ_2 with **(a)** Contour and **(b)** Surface plot.

7 Numerical results

In order to provide empirical evidence to support the theoretical findings obtained in this study, several numerical simulations were conducted. To approximate the solution to the differential equations in the model, we applied the predictor-corrector method in the sense of the Caputo-Fabrizio fractional derivative, which was introduced by Toh et al. [42]. To conduct these simulations, the initial conditions for the model components were set at $S(0) = 0.15$, $E(0) = 0.15$, $I(0) = 0.10$, and $R(0) = 0$.

Additionally, the values of the model parameters were assigned as $\Lambda = 0.25$, $\mu = 0.2$, $\gamma_1 = 0.25$, $\gamma_2 = 0.15$, $c = 0.15$, $b = 0.10$, $\alpha = 0.30$, $\epsilon = 0.30$, and $\beta = 0.5$. By utilizing these initial conditions

and parameter values, the simulations were able to provide insights into the behavior and characteristics of the model under distinct values of the fractional derivative. Through these simulations, it was possible to observe the impact of changes in the parameters and initial conditions on the model's predictions, thus allowing for a more comprehensive analysis of the model's dynamics. The impact of the fractional derivative of Caputo-Fabrizio sensitivity on the components of the influenza model is observed for arbitrarily selected orders, as shown in Figure 3-4. In addition to this, in Figure 5, a detailed explanation of the behavioral responses of exposed and infected individuals at various values of γ_1 and γ_2 contact rates is provided. There is a tendency for the number of exposed and infected individuals to increase when the threshold values for γ_1 and γ_2 contact rates are exceeded. When comparing the simulations in Figure 5 (a) and Figure 5 (b), it can be seen that the γ_1 contact rate is more dominant in the spread of the influenza virus compared to γ_2.

Moreover, this high transmission rate is achieved at lower values of γ_1 than γ_2. This result is also supported by the fact that γ_1 has a lower threshold value than γ_2, as seen in Figure 1 (a)-(b). This finding implies that the interaction with exposed individuals plays a more significant role in the spread of the influenza virus than the interaction with infected individuals.

There could be several reasons for this. One possible explanation is that exposed individuals may be more likely to transmit the virus to others due to their higher viral load or greater susceptibility to infection. Another possible explanation is that the timing of interactions with exposed individuals may be more critical for transmission than interactions with infected individuals. If individuals are more likely to interact with others during the early stages of the disease when they are exposed but not yet showing symptoms, this could contribute to the higher transmission rate among exposed individuals.

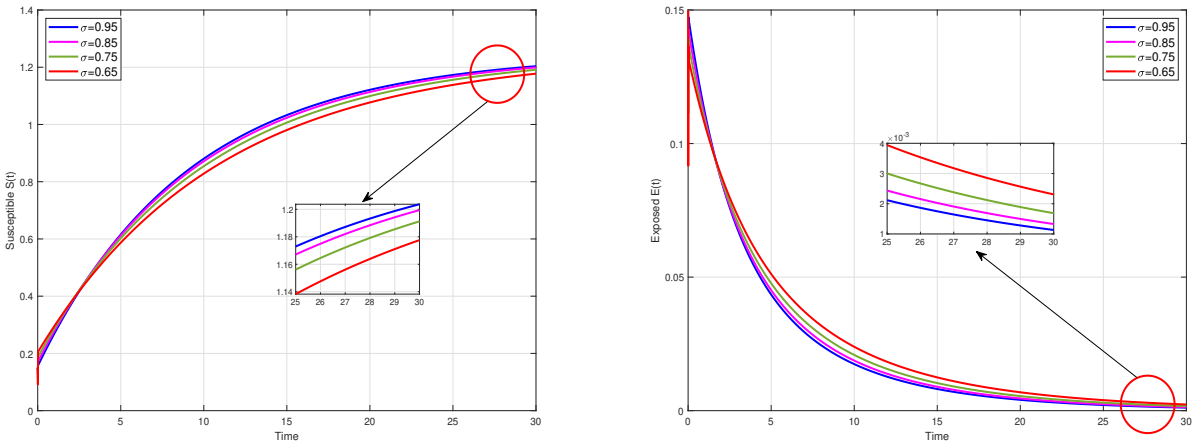

Figure 3. The behavior of the model (2) compartments **(a)** Susceptible and **(b)** Exposed according to the different fractional orders $\sigma = 0.95, 0.85, 0.75, 0.65$.

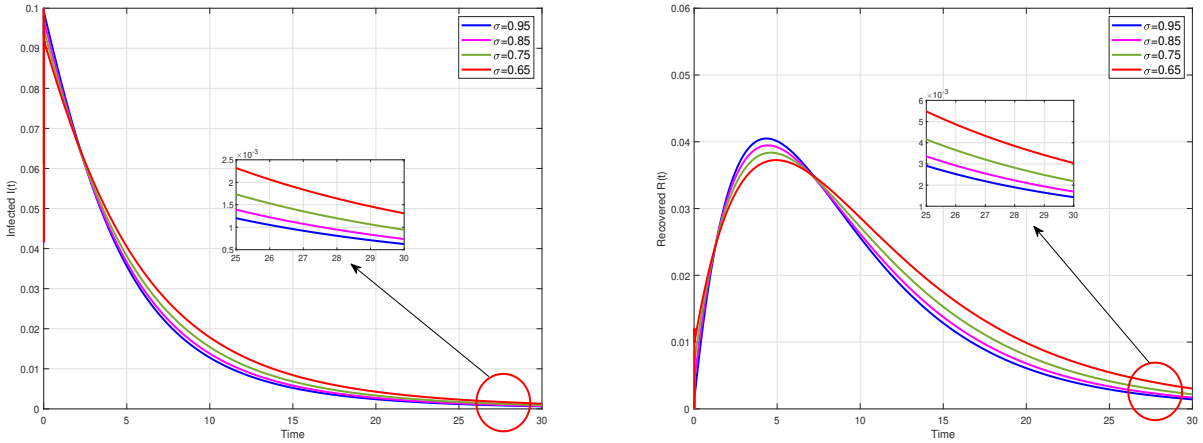

(a) **(b)**

Figure 4. The behavior of the model (2) compartments **(a)** Infected and **(b)** Recovered according to the different fractional orders $\sigma = 0.95, 0.85, 0.75, 0.65$.

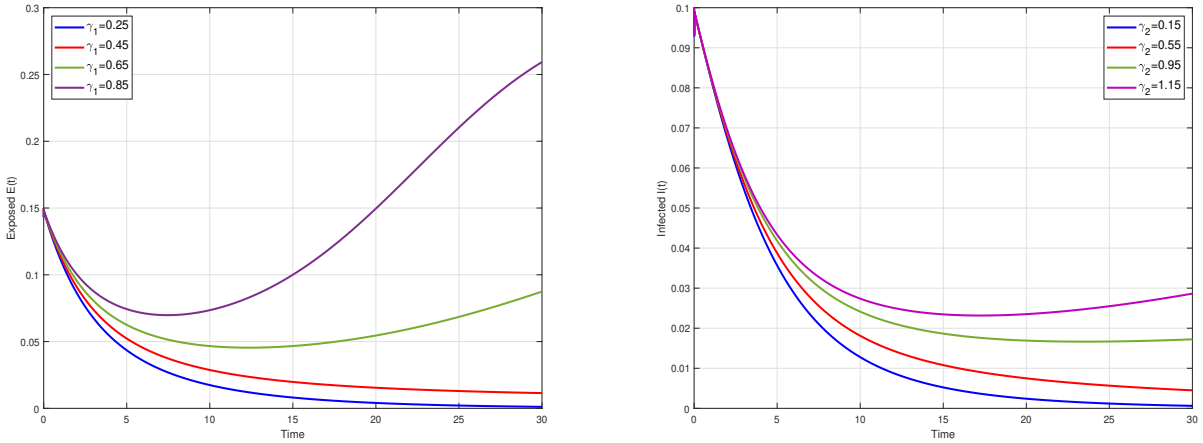

(a) **(b)**

Figure 5. The changes in the **(a)** Exposed $E(t)$ and **(b)** Infected $I(t)$ populations depending on the contact rates of virus transmission γ_1 and γ_2.

8 Conclusion

This manuscript presents a novel approach to modeling influenza A disease dynamics by incorporating the Caputo-Fabrizio fractional derivatives into the model. By considering distinct contact rates for exposed and infected individuals, the study explores the fractional derivative concept and demonstrates its effectiveness in predicting disease dynamics. The reproduction number of the influenza model was obtained and examined to show the effectiveness of different contact rates. In simulations, the γ_1 contact rate with exposed individuals played a more active role in disease spread. It can be thought that the reason for this was still at the beginning of the outbreak. Because, during the early stages of an outbreak, the contact rate with exposed individuals may be more important, as these individuals have not yet developed symptoms or been diagnosed with the disease, and therefore may not be aware that they are contagious. This makes them potentially

more dangerous to the population, as they may be spreading the disease unknowingly. Modeling the contact rate with exposed individuals can help to identify the potential spread of the disease before it is detected by traditional disease surveillance methods. The numerical simulations conducted in this study validate the proposed approach and suggest that the Caputo-Fabrizio fractional derivative can provide valuable insights into the mechanisms underlying influenza A disease. The findings of this study have important implications for improving the accuracy of disease models and developing more effective strategies for controlling the spread of influenza A. In future work, the model will be expanded to consider different incidence rates and further investigations will be conducted to examine the spread of Influenza A disease from different perspectives.

Declarations

Consent for publication

Not applicable.

Conflicts of interest

The authors declare that they have no conflict of interests.

Funding

Not applicable.

Author's contributions

F.E.: Conceptualization, Methodology, Software, Writing - Original Draft, E.U.: Conceptualization, Methodology, Writing - Original Draft, S.U.: Conceptualization, Methodology, Writing - Original Draft, N.O.: Methodology, Writing - Review and Editing. All authors discussed the results and contributed to the final manuscript.

Acknowledgements

Not applicable.

References

[1] Wu, Y., Wu, Y., Tefsen, B., Shi, Y. and Gao, G.F. Bat-derived influenza-like viruses H17N10 and H18N11. *Trends in Microbiology*, 22(4), 183-191, (2014). [CrossRef]

[2] Kilbourne, E.D. Influenza pandemics of the 20th century. *Emerging Infectious Diseases*, 12(1), 9-14, (2006). [CrossRef]

[3] Uçar, E., Ozdemir, N. and Altun, E. Fractional order model of immune cells influenced by cancer cells. *Mathematical Modeling Natural Phenomea*, 14(3), 12, (2019). [CrossRef]

[4] Özköse, F., Şenel, M.T. and Habbireeh, R. Fractional-order mathematical modelling of cancer cells-cancer stem cells-immune system interaction with chemotherapy. *Mathematical Modelling and Numerical Simulation with Applications*, 1(2), 67-83, (2021). [CrossRef]

[5] Uçar, E., Özdemir, N. and Altun, E. Qualitative analysis and numerical simulations of new model describing cancer. *Journal of Computational and Applied Mathematics*, 422, 114899, (2023). [CrossRef]

[6] Qureshi, S., Yusuf, A., Shaikh, A.A. and Inc, M. Transmission dynamics of varicella zoster

virus modeled by classical and novel fractional operators using real statistical data. *Physica A: Statistical Mechanics and its Applications*, 534, 122149, (2019). [CrossRef]

[7] Ahmad, S., Qiu, D. and ur Rahman, M. Dynamics of a fractional-order COVID-19 model under the nonsingular kernel of Caputo-Fabrizio operator. *Mathematical Modelling and Numerical Simulation with Applications*, 2(4), 228-243, (2022). [CrossRef]

[8] Hamou, A.A., Rasul, R.R.Q., Hammouch, Z. and Özdemir, N. Analysis and dynamics of a mathematical model to predict unreported cases of COVID-19 epidemic in Morocco. *Computational and Applied Mathematics*, 41, 289, (2022). [CrossRef]

[9] Okundalaye, O.O., Othman, W.A.M. and Oke, A.S. Toward an efficient approximate analytical solution for 4-compartment COVID-19 fractional mathematical model. *Journal of Computational and Applied Mathematics*, 416, 114506, (2022). [CrossRef]

[10] Koca, İ, Bulut, H. and Akçetin, E. A different approach for behavior of fractional plant virus model. *Journal of Nonlinear Sciences and Applications*, 15(3), 186-202, (2022). [CrossRef]

[11] Uçar, S., Ozdemir, N., Koca, I. and Altun, E. Novel analysis of the fractional glucose–insulin regulatory system with non-singular kernel derivative. *The European Physical Journal Plus*, 135(5), 1-18, (2020). [CrossRef]

[12] Naik, P.A., Eskandari, Z., Yavuz, M. and Zu, J. Complex dynamics of a discrete-time Bazykin-Berezovskaya prey-predator model with a strong Allee effect. *Journal of Computational and Applied Mathematics*, 413, 114401, (2022). [CrossRef]

[13] Evirgen, F. Transmission of Nipah virus dynamics under Caputo fractional derivative. *Journal of Computational and Applied Mathematics*, 418, 114654, (2023). [CrossRef]

[14] Olumide, O.O., Othman, W.A.M. and Ozdemir, N. Efficient solution of fractional-order SIR epidemic model of childhood diseases with optimal homotopy asymptotic method. *IEEE Access*, 10, 9395-9405, (2022). [CrossRef]

[15] Uçar, S. Analysis of hepatitis B disease with fractal-fractional Caputo derivative using real data from Turkey. *Journal of Computational and Applied Mathematics*, 419, 114692, (2023). [CrossRef]

[16] Tajadodi, H., Jafari, H. and Ncube, M.N. Genocchi polynomials as a tool for solving a class of fractional optimal control problems. *An International Journal of Optimization and Control: Theories & Applications (IJOCTA)*, 12(2), 160–168, (2022). [CrossRef]

[17] Chatterjee, A. and Pal, S. A predator-prey model for the optimal control of fish harvesting through the imposition of a tax. *An International Journal of Optimization and Control: Theories & Applications (IJOCTA)*, 13(1), 68–80, (2023). [CrossRef]

[18] Kaliraj, K., Viswanath, K.S., Logeswari, K. and Ravichandran, C. Analysis of Ffractional integro–differential equation with robin boundary conditions using topological degree method. *International Journal of Applied and Computational Mathematics*, 8(4), 176, (2022). [CrossRef]

[19] Manjula, M., Kaliraj, K., Botmart, T., Nisar, K.S. and Ravichandran, C. Existence, uniqueness and approximation of nonlocal fractional differential equation of sobolev type with impulses. *AIMS Mathematics*, 8(2), 4645-4665, (2023). [CrossRef]

[20] Vijayaraj, V., Ravichandran, C., Sawangtong, P. and Nisar, K.S. Existence results of Atangana-Baleanu fractional integro-differential inclusions of Sobolev type. *Alexandria Engineering Journal*, 66, 249-255, (2023). [CrossRef]

[21] Sene, N. Theory and applications of new fractional-order chaotic system under Caputo Operator. *An International Journal of Optimization and Control: Theories & Applications (IJOCTA)*, 12(1), 20-38, (2022). [CrossRef]

[22] Koca, I. Modeling the heat flow equation with fractional-fractal differentiation. *Chaos, Solitons & Fractals*, 128, 83-91, (2019). [CrossRef]

[23] Alexander, M.E., Bowman, C., Moghadas, S.M., Summers, R., Gumel, A.B. and Sahai, B.M. A vaccination model for transmission dynamics of influenza. *SIAM Journal on Applied Dynamical Systems*, 3(4), 503-524, (2004). [CrossRef]

[24] Casagrandi, R., Bolzoni, L., Levin, S.A. and Andreasen, V. The SIRC model and influenza A. *Mathematical Biosciences*, 200(2), 152-169, (2006). [CrossRef]

[25] Iwami, S., Takeuchi, Y. and Liu, X. Avian–human influenza epidemic model. *Mathematical Biosciences*, 207(1), 1-25, (2007). [CrossRef]

[26] Tracht, S.M., Del Valle, S.Y. and Hyman, J.M. Mathematical modeling of the effectiveness of facemasks in reducing the spread of novel influenza A (H1N1). *PloS One*, 5(2), e9018, (2010). [CrossRef]

[27] González-Parra, G., Arenas, A.J. and Chen-Charpentier, B.M. A fractional order epidemic model for the simulation of outbreaks of influenza A (H1N1). *Mathematical Methods in the Applied Sciences*, 37(15), 2218-2226, (2014). [CrossRef]

[28] Khanh, N.H. Stability analysis of an influenza virus model with disease resistance. *Journal of the Egyptian Mathematical Society*, 24, 193-199, (2016). [CrossRef]

[29] Jia, J. and Xiao, J. Stability analysis of a disease resistance SEIRS model with nonlinear incidence rate. *Advances in Difference Equations*, 75, (2018). [CrossRef]

[30] Quirouette, C., Younis, N.P., Reddy, M.B. and Beauchemin, C.A. A mathematical model describing the localization and spread of influenza A virus infection within the human respiratory tract. *PLoS Computational Biology*, 16(4), e1007705, (2020). [CrossRef]

[31] Srivastava, H.M., Saad, K.M., Gómez-Aguilar, J.F. and Almadiy, A.A. Some new mathematical models of the fractional-order system of human immune against IAV infection. *Mathematical Biosciences and Engineering*, 17(5), 4942-4969, (2020). [CrossRef]

[32] Baba, I.A., Ahmad, H., Alsulami, M.D., Abualnaja, K.M. and Altanji, M. A mathematical model to study resistance and non-resistance strains of influenza. *Results in Physics*, 26, 104390, (2021). [CrossRef]

[33] Ojo, M.M., Benson, T.O., Peter, O.J. and Goufo, E.F.D. Nonlinear optimal control strategies for a mathematical model of COVID-19 and influenza co-infection. *Physica A: Statistical Mechanics and its Applications*, 607, 128173, (2022). [CrossRef]

[34] Etemad, S., Avci, I., Kumar, P., Baleanu, D. and Rezapour, S. Some novel mathematical analysis on the fractal–fractional model of the AH1N1/09 virus and its generalized Caputo-type version. *Chaos, Solitons & Fractals*, 162, 112511, (2022). [CrossRef]

[35] Derradji, L.S., Hamidane, N. and Aouchal, S. A fractional SEIRS model with disease resistance and nonlinear generalized incidence rate in Caputo–Fabrizio sense. *Rendiconti del Circolo Matematico di Palermo Series 2*, 72(1), 81-98, (2023). [CrossRef]

[36] Sabir, Z., Said, S.B. and Al-Mdallal, Q. A fractional order numerical study for the influenza disease mathematical model. *Alexandria Engineering Journal*, 65, 615-626, (2023). [CrossRef]

[37] Caputo, M. and Fabrizio, M. A new definition of fractional derivative without singular kernel. *Progress in Fractional Differentiation and Applications*, 1, 73-85, (2015). [CrossRef]

[38] Atangana, A. and Talkahtani, B.S. Extension of the resistance, inductance, capacitance electrical circuit to fractional derivative without singular kernel. *Advances in Mechanical Engineering*,

7, 1-6, (2015). [CrossRef]

[39] Gomez-Aguilar, J.F., Rosales-García, J.J. and Bernal-Alvarado, J.J. Fractional mechanical oscillators. *Revista Mexicana Física*, 58, 348-352, (2012). [CrossRef]

[40] Driessche, V.P. and Watmough, J. Reproduction numbers and sub-threshold endemic equilibria for compartmental models of disease transmission. *Mathematical Biosciences*, 180(2), 29-48, (2002). [CrossRef]

[41] Diekmann, O., Heesterbeek, J.A.P. and Roberts, M.G. The construction of next-generation matrices for compartmental epidemic models. *Journal of the Royal Society Interface*, 7(47), 873-885, (2010). [CrossRef]

[42] Toh, Y.T., Phang, C. and Loh, J.R. New predictor-corrector scheme for solving nonlinear differential equations with Caputo-Fabrizio operator. *Mathematical Methods in the Applied Sciences*, 42, 175-185, (2019). [CrossRef]

Mathematical Modelling and Numerical Simulation with Applications (MMNSA)
(https://dergipark.org.tr/en/pub/mmnsa)

How to cite this article: Evirgen, F., Uçar, E., Uçar, S. & Özdemir, N. (2023). Modelling Influenza A disease dynamics under Caputo-Fabrizio fractional derivative with distinct contact rates. *Mathematical Modelling and Numerical Simulation with Applications*, 3(1), 58-73. https://doi.org/10.53391/mmnsa.1274004